INTERNATIONAL JOURNAL OF OPTIMIZATION IN CIVIL ENGINEERING
Int. J. Optim. Civil Eng., 2020; 10(3):531-551

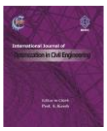

RELIABILITY ASSESSMENT OF TRANSMISSION LINE TOWERS USING METAHEURISTIC ALGORITHMS

P. Hosseini[1*, †], S. R. Hoseini Vaez[2], M.A. Fathali[2] and H. Mehanpour[2]
[1]*Faculty of Engineering, Mahallat Institute of Higher Education, Mahallat, Iran*
[2]*Department of Civil Engineering, Faculty of Engineering, University of Qom, Qom, Iran*

ABSTRACT

Due to the random nature of the variables affecting the analysis and design of structures, the reliability method is considered as one of the most important and widely used topics in structural engineering. Despite the simplicity of moment methods, the answer to problems with multiple design points (the point with the highest probability of failure) such as transmission line towers depends a lot on the starting point of the search; and it may converge to the local optima answer which is not desirable. Simulation methods also require a large number of evaluations of the limit state function and increase the volume and time of calculations. Also, the design point is not calculated in most of these methods. In this study, the reliability index of four transmission line towers was calculated with four metaheuristic algorithms in which the limit state function was defined based on the displacement of nodes and the results were compared with the results of Monte Carlo Simulation (MCS) method. For this purpose, the objective function was defined as the geometric distance between the point on the function of the boundary condition to the origin in the standard normal coordinate system and the constraint of the problem (the limit state function) based on the displacement of the nodes. Random variables in these problems consisting of the cross-sectional area of the members, the modulus of elasticity, and the nodal loads.

Keywords: transmission line towers; reliability index; truss structures; metaheuristic algorithms.

Received: 19 April 2020; Accepted: 16 July 2020

1. INTRODUCTION

The optimal design of structures, which often aims to provide the minimum weight of the

[*]Corresponding author: Faculty of Engineering, Mahallat Institute of Higher Education, Mahallat, Iran
[†]E-mail address: P.Hosseini@mahallat.ac.ir (P. Hosseini)

structure, leads to the use of the maximum capacity of the members. Since there are always uncertainties in structural parameters such as material properties, external loads, cross-sectional geometric characteristics of the members, geometric dimensions of the structure, etc., the safety of the optimal design may be questioned. Therefore, in order to consider this issue, the reliability method has recently been seriously considered. Using the reliability method in structural systems, the uncertainties caused by the statistical nature of structural parameters can be turned into mathematical equations and safety considerations can be slightly incorporated into the design process [1-5]. Assessing the probability of failure or calculating the reliability index is a key issue in analyzing the reliability of structures. Over the past decades, researchers have proposed a number of different methods for calculating the probability of failure or the reliability index, which can be divided into three categories: moment methods, simulation method, and metaheuristic methods.

In Moment methods, using the gradient of the limit state function, the shortest distance of this function from the center of the standard normal coordinate system is defined as the reliability index and then the probability of failure is obtained by having this index. In these methods, the calculation of the first and second-order derivatives (such as FORM and SORM methods, respectively) are required for the limit state function [6-8]. In simulation methods such as Monte Carlo simulation (MCS), after producing random samples based on the probability density function of sampling for random variables, the limit state function for each sample is calculated. The probability of failure is obtained by dividing the number of samples that the limit state function has become negative by the total number of simulation samples [9-13]. In metaheuristic methods, the problem of calculating the reliability index becomes a constrained optimization problem. In these methods, the shortest distance of the limit state function from the center of the standard coordinate system is considered as the objective function and the problem constraint is also considered as the limit state function [14-21].

Despite the simplicity of moment methods, the answer to the problem depends a lot on the starting point of the search, and also in problems with multiple design points, it may converge to the local optima answer which is not desirable. In contrast, meta-heuristic methods have the ability to exit the local optima and are independent of the initial values of the search points. Simulation methods also require a large number of simulations (especially for low-probability failures) and therefore, the high volume of the evaluation depends on the limit conditions. In addition, the point with the highest probability of failure (design point) is not calculated, which is calculated in metaheuristic methods.

By combining metaheuristic methods with form method, it is possible to assess the reliability index of problems whose limit state functions are not available in the form of explicit mathematical formulas [22]. Transmission line towers do not have an explicit mathematical form. So, using metaheuristic algorithms is a suitable solution to calculate the reliability index of these types of problems. In this study, four population-based meta-algorithmic algorithms including CBO, ECBO, VPS and EVPS are used to calculate the reliability index of four power transmission line towers. Probabilistic constraints are expressed on the basis of nodal displacement. It should be noted that 30 independent runs are performed for each algorithm in each problem, and the results are compared.

This study is organized as follows:

In the first section, the introduction is presented. A brief explanation of four

metaheuristic algorithms is presented in section 2 and a brief statement about the reliability index is presented in section 3. Section 4 consists of four well-known power transmission line towers and finally, the concluding remarks are presented in section 5.

2. RELIABILITY ASSESSMENT

The performance of any structure can be expressed by a function (consisting of basic random variables) that called the Limit State Function (LSF). So that the positive and negative value of the LSF indicates safety and failure region, respectively. In analyzing a system, the failure region is expressed as the following equation:

$$g(R,Q) = R - Q \le 0 \tag{1}$$

where R and Q are the value of resistance and load effect on structure, respectively. The probability of structural failure can be presented by considering the joint probability density function, $f_{R,Q}$, for the random variables of R and Q as follows:

$$P_f = P\{g(R,Q) \le 0\} = \int_{g \le 0} f_{R,Q}\, dR\, dQ \tag{2}$$

where P_f is the probability of failure. It is very difficult to obtain a direct answer to this equation due to the complexity of the joint probability density function (especially for variables with non-normal distribution) and in most cases, it is performed using simplistic assumptions. These assumptions are based on two approximate methods and a simulation method. Approximate methods are established on the reliability index use the first and second-order Taylor expansion of the limit state function. Simulation-based methods calculate the probability of failure directly and using sampling.

According to the definition provided by Hasofer and Lind [23], the design point is a point on the limit state function with g=0 that this point has the least distance from the origin in the standard normal space. This point is also known as the point with the most probable failure. The distance from this point to the source is considered as a reliability index, which allows $P_f = \Phi(-\beta)$ to estimate the probability of structural failure (where Φ is the standard normal cumulative distribution function). So, in order to calculate the design point, it is necessary to use the optimization problem according to equation (3).

$$\begin{aligned} &\textit{Find} && U = \{u_1, u_2, u_3, ..., u_n\} \\ &\textit{Min} && \beta = \sqrt{\sum_{i=1}^{n} u_i^{\,2}} = \sqrt{u^t u} = \sqrt{u_1^2 + u_2^2 + u_3^2 + ... + u_n^2} \\ &\textit{Subject to} && g(U) = 0 \end{aligned} \tag{3}$$

where u_i presents the value of the ith random variable in the standard normal space and n

shows the number of random variables. This parameter is calculated for random variables with normal distribution through equation (4).

$$u_i = \frac{x_i - \mu_{x_i}}{\sigma_{x_i}} \tag{4}$$

In above Eq. (4), μ_{xi} and σ_{xi} are the mean and standard deviation of x_i random variable, respectively. In this study, in order to apply the type of distribution of variables, the search space for the optimization problem for n samples of each variable is generated according to the pseudo-code shown in Fig. 1. Metaheuristic algorithm creates a vector whose dimension is the total number of random variables (N_{RV}) of the integers in the range [1,n] for the search of the optimal answer. It should be noted that the vector U (in Eq. (3)) is created from the search space of the problem.

for i=1:N_{RV}
  Generate the n-dimensional **Rand** vector in the interval of [0, 1] randomly.
  Convert the **Rand** vector to $\mathbf{S_i}$ vector by standard normal distribution (μ=0, σ=1).
  Generate distribution of the i^{th} random variable according to following equation: $\mathbf{X_i} = \mu_{xi} + \sigma_{xi} . \mathbf{S_i}$
  Ascending sorting of $\mathbf{X}_i$ and store it in the i^{th} row of **SearchSpace** matrix.
end

Figure 1. Pseudo-code of generating the search space

3. METAHEURISTIC ALGORITHMS

In this section six metaheuristic algorithms are briefly presented as follows:

3.1 Colliding bodies optimization

Colliding Bodies Optimization (CBO) algorithm was introduced by Kaveh and Mahdavi [24]. This algorithm is based on a one-dimensional collision between two bodies with each agent being modeled as an object. Initial agents are generated randomly in a permissible range. The next steps is performed according to velocities and the masses of each agent.

3.2 Enhanced colliding bodies optimization

Enhanced colliding bodies optimization (ECBO) algorithm was introduced by Kaveh and Ilchi Ghazaan [25] in order to improve the CBO performance. This algorithm uses memory to enhance the convergence rate of the CBO algorithm. The new population is sorted in ascending order according to the values of their objective function. Finally, the new position of moving and stationary CBs is calculated similarly to CBO algorithm.

3.3 Vibrating particles system algorithm

Vibrating Particles Systems (VPS) algorithm was developed by Kaveh and Ilchi Ghazaan [26]. This method is adapted from the free vibration of single degree of freedom systems with viscous damping so that each answer is modeled as a particle that moves to its

equilibrium position. New positions are updated according to a historically best position.

3.4 Enhanced vibrating particles system

Enhanced Vibrating Particles System (EVPS) is a modified version of the VPS algorithm that was presented by Kaveh et al. [27-29]. This algorithm employs some new approaches to gaining the optimum answer.

4. NUMERICAL PROBLEMS

In this section, the reliability index of four transmission line towers that optimized (weight optimization) by other researchers, is determined using metaheuristic algorithms, and their results are presented. The reliability index in all examples is calculated based on node displacement probability constraints. Random variables considered in all problems are consisting of: modulus of elasticity (E), external load (P) and cross-sectional area (A) of the elements (the group of elements). All random variables have a normal distribution with a coefficient of variation of 5%. To ensure the performance of the algorithms, the reliability index for each of the problems was obtained by all of the algorithms in 30 independent runs. The population size and the maximum number of iterations of all algorithms are 30 and 1000, respectively. The number of considered samples (n) for each random variable in all problems is 10^6. Also, in order to measure the accuracy of algorithms in calculating the reliability index, this index has been estimated 30 times in each problem using the Monte Carlo simulation (MCS) method, which is a common method for calculating the reliability index. The average of MCS results obtained for each problem has been reported as MCS reliability index. It should be noted that the number of MCS samples in all cases is 2×10^5.

4.1 A 25-bar planar truss

The first problem is the 25-member truss shown in Fig. 2. This truss is a well-known example that has been studied by many researchers [28, 30]. The modulus of elasticity (E) and the of material (ρ) is 68950 MPa and 2767.990 kg / m^3, respectively. The members of this truss are divided into eight groups. The cross-sectional area of the elements group has been selected according to the optimal design of Ho-Huu et al. [31]. The grouping of elements and their cross-sections are shown in Table 1 and the loading of this problem is also presented in Table 2. The number of random variables in this problem is 13 variables. The reliability index for probabilistic constraints is the displacement of the first node in Y direction (less than allowable value equal to 0.635 cm).

Fig. 3 shows the performance of the algorithms in 30 independent runs. Diagrams show the ratio of the best total response to each run solution in descending order for each algorithm. The higher the ratio, means the smaller difference between the best answer and the obtained answers which means the better answer is achieved. As shown in this figure, the performance of the EVPS algorithm is more uniform and appropriate relative to other algorithms. The convergence trend of the best response and the average response of each algorithm are shown in Figs. 4 and 5, respectively. The design point, the best, the worst, and the average of the answers of each algorithm and the value of the reliability index obtained

from the MCS method for this problem are reported in Table 3. This table shows that the ability of the EVPS algorithm to find the optimal answer (calculating the reliability index) is higher than other algorithms and also, this algorithm has found an answer with an acceptable difference compared to the MCS method.

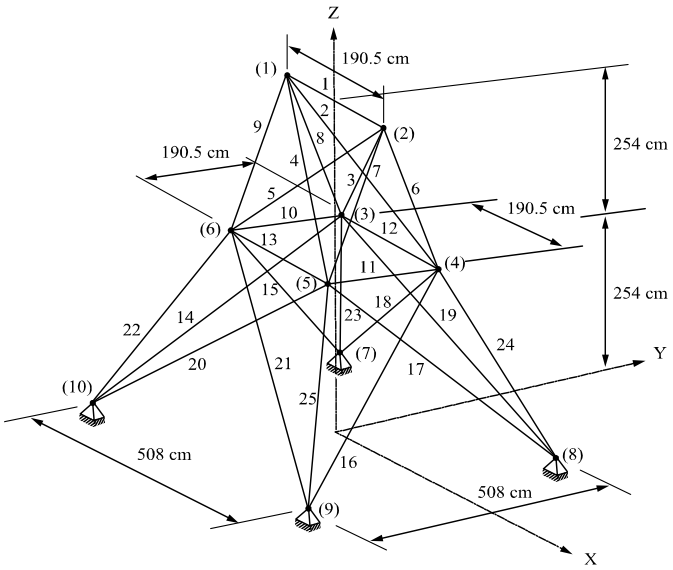

Figure 2. Schematic of the 25-member truss

Table 1: Element grouping adopted in the 25-member truss

Group number	Element	Cross section(cm^2)
1	1	0.6452
2	2-5	12.9032
3	6-9	21.9454
4	10-11	0.6452
5	12-13	0.6452
6	14-17	7.7419
7	18-21	12.2580
8	22-25	21.9454

Table 2: Loading of the 25-member truss

Node	Force in X-direction (kN)	Force in Y-direction (kN)	Force in Z-direction (kN)
1	*P1*= 4.45	*P2*= -44.5	*P2*= -44.5
2	0.0	*P2*= -44.5	*P2*= -44.5
3	*P3*= 2.67	0.0	0.0
6	*P4*= 44.5	0.0	0.0

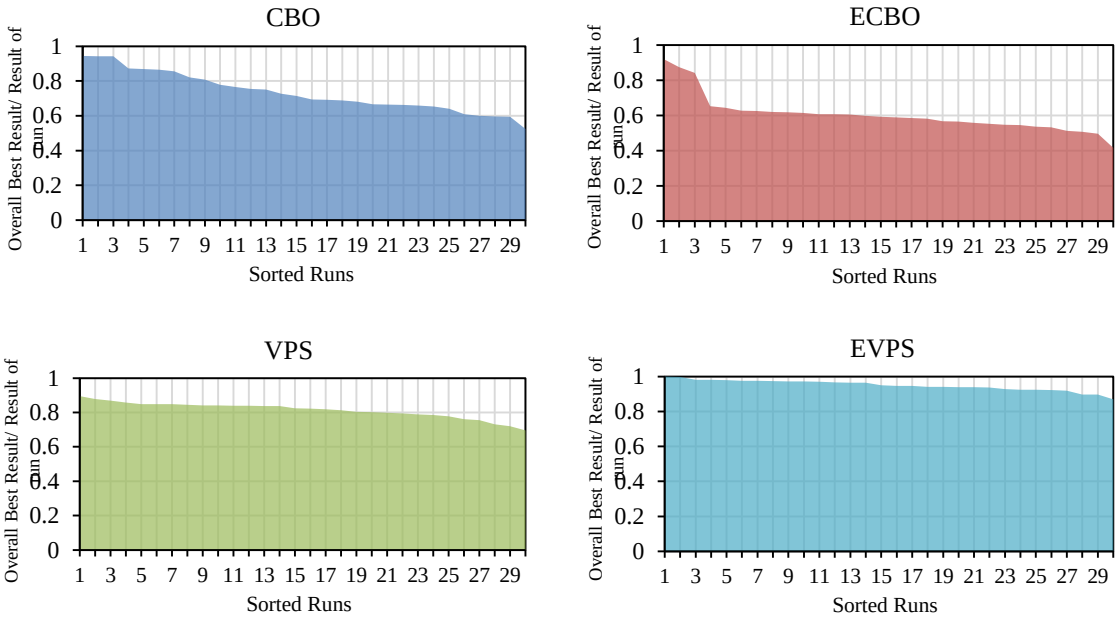

Figure 3. Comparison of the results of all algorithms in 30 independent runs for the 25-member truss problem

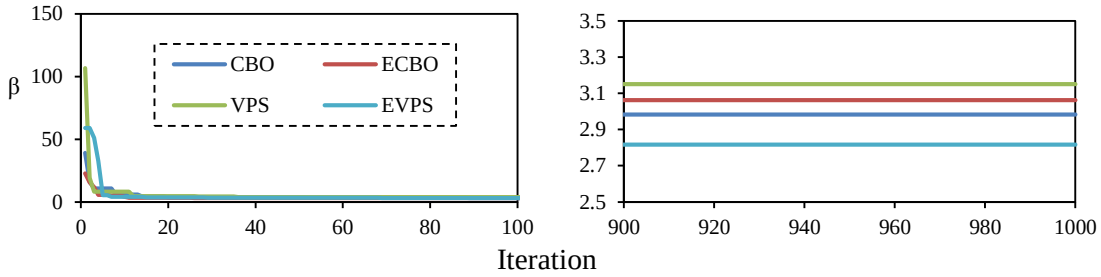

Figure 4. Comparison of convergence trend of the best run of each algorithm for the 25-member truss problem

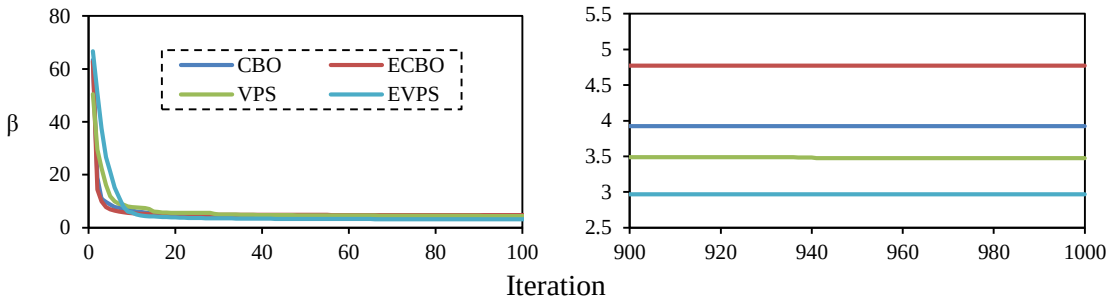

Figure 5. Comparison of the convergence trend of the average runs of each algorithm for the 25-member truss problem

Table 3: Optimization results obtained by algorithms for the 25-member truss

Random variables of the design point	EVPS	VPS	ECBO	CBO	MSC
A1 (cm2)	0.6452	0.6642	0.6452	0.6452	–
A2 (cm2)	12.7782	12.8380	13.1661	12.8586	–
A3 (cm2)	21.3179	21.2309	22.2351	21.0335	–
A4 (cm2)	0.6452	0.6335	0.6452	0.6455	–
A5 (cm2)	0.6449	0.6518	0.6476	0.6447	–
A6 (cm2)	7.6275	7.5750	7.7178	7.4755	–
A7 (cm2)	12.0741	12.3773	11.7870	12.1013	–
A8 (cm2)	20.9850	21.7816	21.1032	21.9154	–
E (MPa)	62081.2390	60430.3072	62947.1023	61243.1039	–
P1 (kN)	4.4482	4.3831	4.4482	4.4524	–
P2 (kN)	48.1270–	47.6890–	49.4167–	48.1212–	–
P3 (kN)	2.2207	2.2334	2.2135	2.2297	–
P4 (kN)	2.6703	2.6883	2.6639	2.6764	–
Best β	2.8172	3.1504	3.0625	2.9830	–
Average β	2.9689	3.4732	4.7731	3.9241	2.7860
Worst β	3.2391	4.0452	6.7710	5.3638	–
Standard deviation β	0.0990	0.2100	0.7200	0.6003	0.0140

4.2 The 47-bar transmission line tower truss

The second problem is the 47-member truss shown in Fig. 6. This truss is a well-known example that has been studied by many researchers [32-36]. The modulus of elasticity (E) and the density of material (ρ) is 206842 MPa and 8303.971 kg / m3, respectively. The members of this truss are divided into 27 groups. The cross-sectional area of the element group has been selected according to the optimal design of Lee et al. [37]. The grouping of elements and their cross-sections are shown in Table 4. P_1 and P_2 loads in X and Y directions that are equal to 26.69 and -62.28kN have been applied to 17 and 22 nodes, respectively. The number of random variables in this problem is 30 variables. The reliability index for probabilistic constraints is the displacement of the 22th node in Y direction (less than allowable value equal to 3.556 cm).

Fig. 7 shows the performance of the algorithms in 30 independent runs. Diagrams show the ratio of the best total response to each run solution in descending order for each algorithm. The higher the ratio, means the smaller difference between the best answer and the obtained answers which means the better answer is achieved. As shown in this figure, the performance of the EVPS algorithm is more uniform and appropriate relative to other algorithms. The convergence trend of the best response and the average response of each algorithm are shown in Figs. 8 and 9, respectively. The design point, the best, the worst, and the average of the answers of each algorithm and the value of the reliability index obtained from the MCS method for this problem are reported in Table 5. This table shows that the

ability of the EVPS algorithm to find the optimal answer (calculating the reliability index) is higher than other algorithms and also, this algorithm has found an answer with an acceptable difference compared to the MCS method.

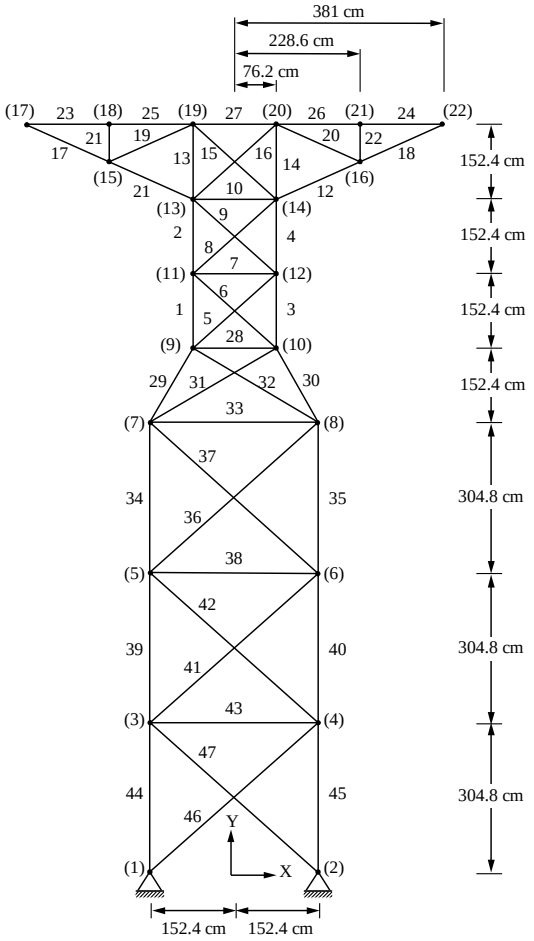

Figure 6. Schematic of the 47-member truss

Table 4: Element grouping adopted in the 47-member truss

Group number	Element	Cross section(cm^2)	Group number	Element	Cross section(cm^2)
1	1 and 3	24.7741	15	27	9.4000
2	2 and 4	21.8064	16	28	2.8516
3	5 and 6	5.0645	17	29 and 30	23.4193
4	7	1.6129	18	31 and 31	9.4000
5	8 and 9	6.4129	19	33	2.5226
6	10	11.6129	20	34 and 35	19.9354
7	11 and 12	13.7419	21	36 and 37	9.4000

Group number	Element	Cross section(cm^2)	Group number	Element	Cross section(cm^2)
8	13 and 14	7.9226	22	38	1.6129
9	15 and 16	10.0839	23	39 and 40	24.7741
10	17 and 18	13.7419	24	41 and 42	10.0839
11	19 and 20	0.7161	25	43	0.7161
12	21 and 22	0.7161	26	44 and 45	29.6128
13	23 and 24	11.6129	27	47 and 48	9.4000
14	25 and 26	11.6129			

Table 5: Optimization results obtained by algorithms for the 25-member truss

Random variables of the design point	EVPS	VPS	ECBO	CBO	MSC
A1 (cm2)	24.4276	25.1873	23.2010	25.4704	-
A2 (cm2)	21.6092	22.0511	21.3762	20.8211	-
A3 (cm2)	5.0607	5.2765	5.0610	5.0609	-
A4 (cm2)	1.6122	1.5716	1.6229	1.6016	-
A5 (cm2)	6.4095	6.7462	6.4222	6.4121	-
A6 (cm2)	11.5957	11.7736	11.6785	11.5356	-
A7 (cm2)	13.6637	13.7179	13.6125	13.4329	-
A8 (cm2)	7.8487	7.6164	7.9311	7.7686	-
A9 (cm2)	9.9102	9.9441	9.6817	10.5952	-
A10 (cm2)	13.5305	13.8445	13.4676	12.7349	-
A11 (cm2)	0.7162	0.7261	0.7143	0.7161	-
A12 (cm2)	0.7158	0.6998	0.7172	0.7161	-
A13 (cm2)	11.5400	11.9515	11.2896	11.9997	-
A14 (cm2)	11.5158	11.4353	11.7880	11.6637	-
A15 (cm2)	9.3403	9.3215	9.5034	9.2583	-
A16 (cm2)	2.8596	2.8695	2.8504	2.8150	-
A17 (cm2)	22.8265	23.4635	22.8067	21.7346	-
A18 (cm2)	9.2168	9.5107	9.3513	9.1072	-
A19 (cm2)	2.5118	2.5196	2.5205	2.3305	-
A20 (cm2)	19.7107	20.0182	19.4822	19.1621	-
A21 (cm2)	9.3978	9.5989	9.4274	9.4210	-
A22 (cm2)	1.6126	1.5177	1.6153	1.6131	-
A23 (cm2)	24.2811	24.5860	24.1635	25.8961	-
A24 (cm2)	10.0804	9.8630	9.9881	10.0864	-

Random variables of the design point	EVPS	VPS	ECBO	CBO	MSC
A25 (cm2)	0.7160	0.7061	0.7141	0.7152	-
A26 (cm2)	29.1402	28.2740	30.8329	29.8953	-
A27 (cm2)	9.3994	9.4744	9.3391	9.4005	-
E (MPa)	176424.1872	175892.8507	183859.5074	171397.5401	-
P1 (kN)	28.2745	28.2267	29.9512	27.4738	-
P2 (kN)	-64.3075	-65.8250	-65.2381	-62.7895	-
P3 (kN)	3.4135	4.6423	4.8649	4.0492	-
P4 (kN)	3.6137	5.5755	6.3949	5.2810	3.3146
Best β	4.3556	6.5961	8.6674	6.2766	-
Average β	0.1995	0.5192	0.9661	0.5380	0.03141
Worst β	24.4276	25.1873	23.2010	25.4704	-
Standard deviation β	21.6092	22.0511	21.3762	20.8211	-

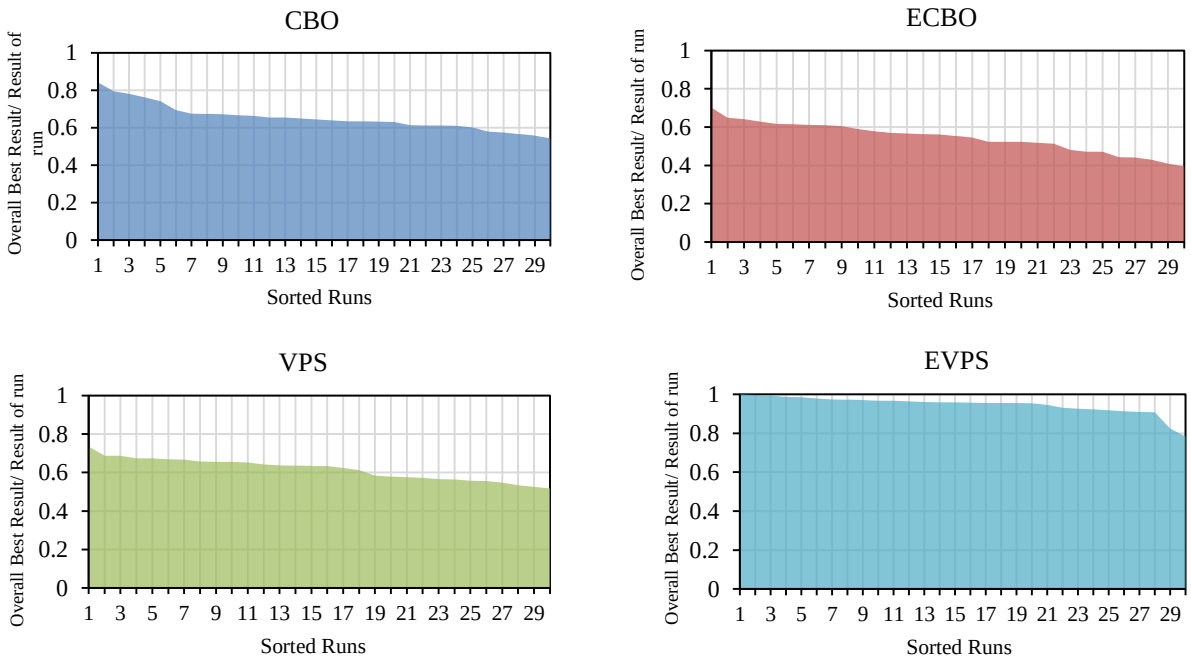

Figure 7. Comparison of the results of all algorithms in 30 independent runs for the 47-member truss problem

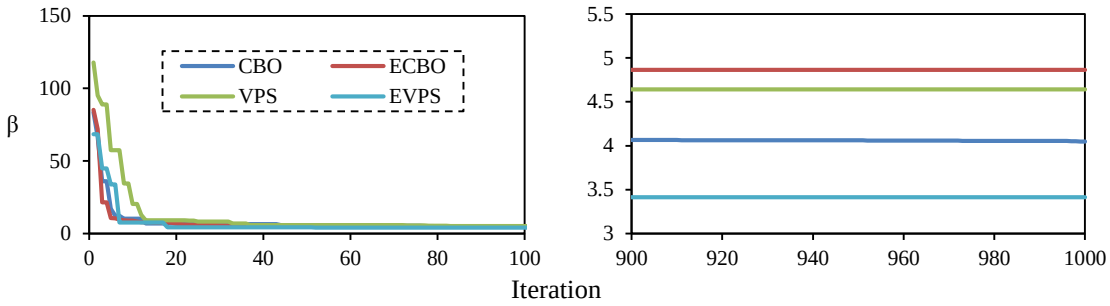

Figure 8. Comparison of convergence trend of the best run of each algorithm for the 47-member truss problem

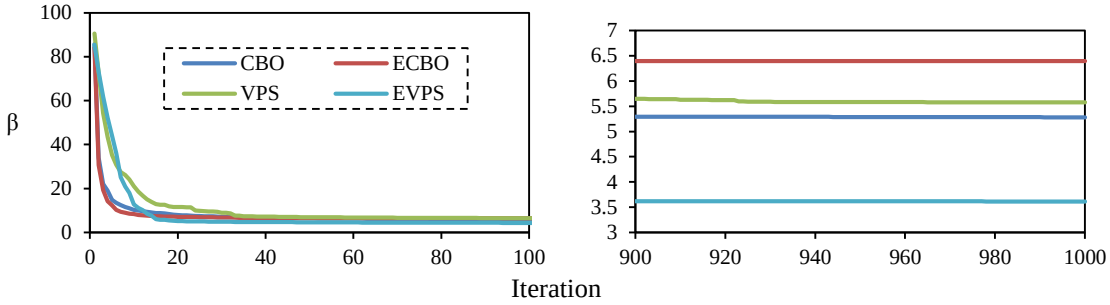

Figure 9. Comparison of convergence trend of the average runs of each algorithm for the 47-member truss problem

4.3 The 160-bar transmission line tower truss

The third problem is the 160-member truss shown in Fig. 10. This truss is a well-known example that has been studied by many researchers [38-42]. The modulus of elasticity (E) and the density of material (ρ) is 200800 MPa and 7850 kg / m3, respectively. The members of this truss are divided into 38 groups. The cross-sectional area of the elements group has been selected according to the optimal design of Groenwold and Stander [43]. The grouping of elements and their cross-sections are shown in Table 6. The loading condition is shown in Table 7. The number of random variables in this problem is 44 variables. The reliability index for probabilistic constraints is the displacement of the 25th node in X direction (less than allowable value equal to 2.4 cm).

Fig. 11 shows the performance of the algorithms in 30 independent runs. Diagrams show the ratio of the best total response to each run solution in descending order for each algorithm. The higher the ratio, means the smaller difference between the best answer and the obtained answers which means the better answer is achieved. As shown in this figure, the performance of the EVPS algorithm is more uniform and appropriate relative to other algorithms. The convergence trend of the best response and the average response of each algorithm are shown in Figs. 12 and 13, respectively. The design point, the best, the worst, and the average of the answers of each algorithm and the value of the reliability index obtained from the MCS method for this problem are reported in Table 8. This table shows that the ability of the EVPS algorithm to find the optimal answer (calculating the reliability index) is higher than other algorithms and also, this algorithm has found an answer with an acceptable difference compared to the MCS method.

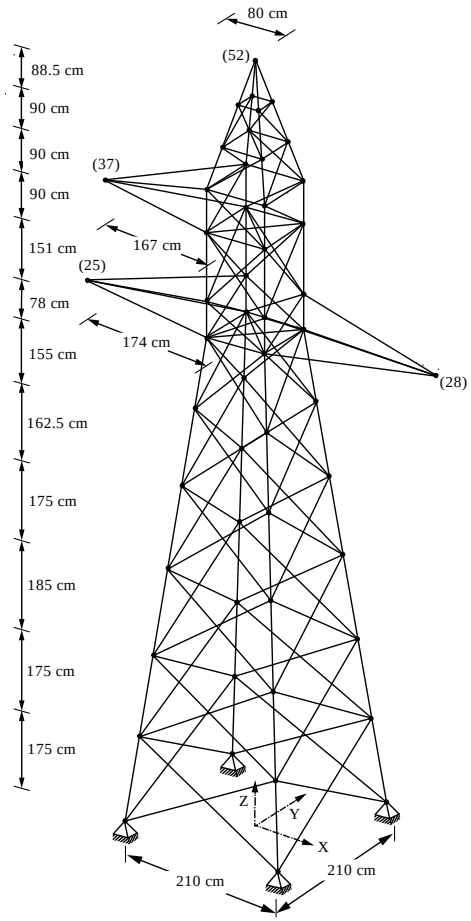

Figure 10. Schematic of the 160-member truss

Table 6: Element grouping adopted in the 160-member truss

Group number	Cross section(cm^2)	Group number	Cross section(cm^2)	Group number	Cross section(cm^2)
1	19.03	14	5.75	27	4.79
2	5.27	15	2.66	28	2.66
3	19.03	16	7.44	29	3.47
4	5.27	17	1.84	30	1.84
5	19.03	18	8.66	31	2.26
6	5.75	19	2.66	32	3.88
7	17.03	20	3.07	33	1.84
8	6.25	21	2.66	34	1.84
9	13.79	22	8.06	35	3.88
10	6.25	23	5.27	36	1.84
11	5.75	24	7.44	37	1.84
12	12.21	25	6.25	38	3.88
13	6.84	26	1.84		

Table 7: Loading of the 160-member truss

Node	Force in X Direction (kN)	Force in Y Direction (kN)	Force in Z Direction (kN)
25	*P1*= -10.699	0.0	*P2*= -5.354
28	*P1*= -10.699	0.0	*P2*= -5.354
37	*P3*= -9.767	0.0	*P2*= -5.354
52	*P4*= -8.512	0.0	*P5*= -4.815

Table 8: Optimization results obtained by algorithms for the 160-member truss

Random variables of the design point	EVPS	VPS	ECBO	CBO	MSC
Best β	3.4082	5.3272	4.3188	3.5917	-
Average β	3.6517	6.2585	6.4290	5.2182	3.2260
Worst β	4.4329	7.6047	7.7111	6.4327	-
Standard deviation β	0.2262	0.4916	0.9338	0.8027	0.0225

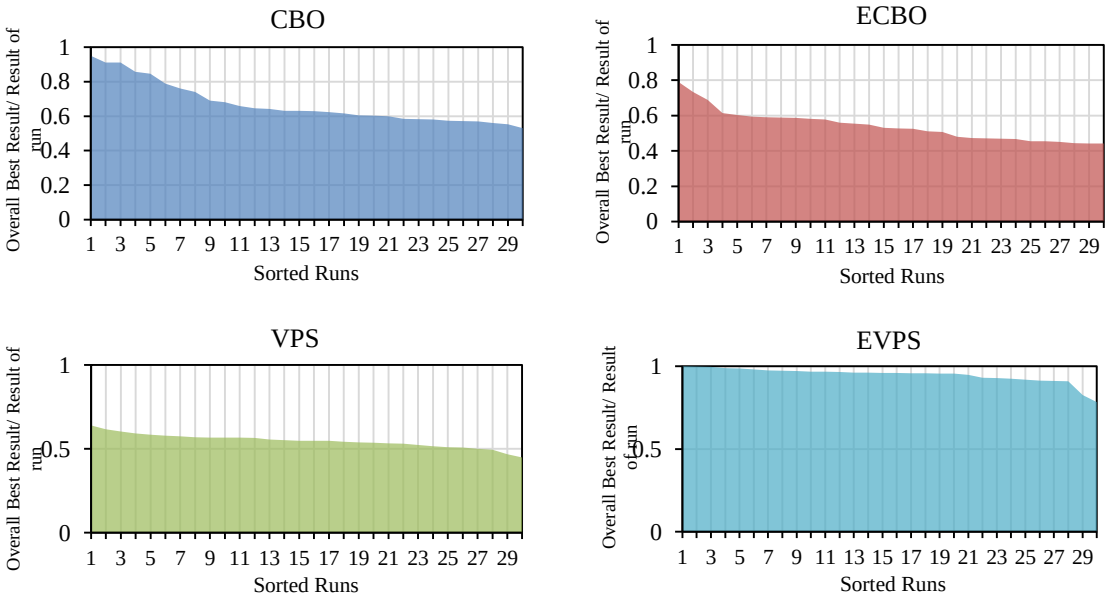

Figure 11. Comparison of the results of all algorithms in 30 independent runs for the 160-member truss problem

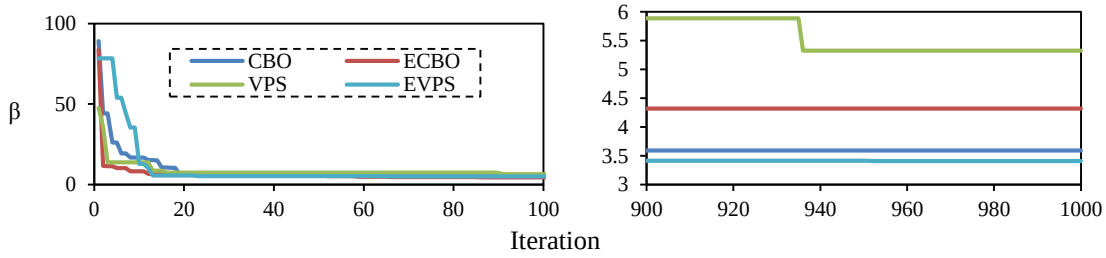

Figure 12. Comparison of the convergence trend of the best run of each algorithm for the 160-member truss problem

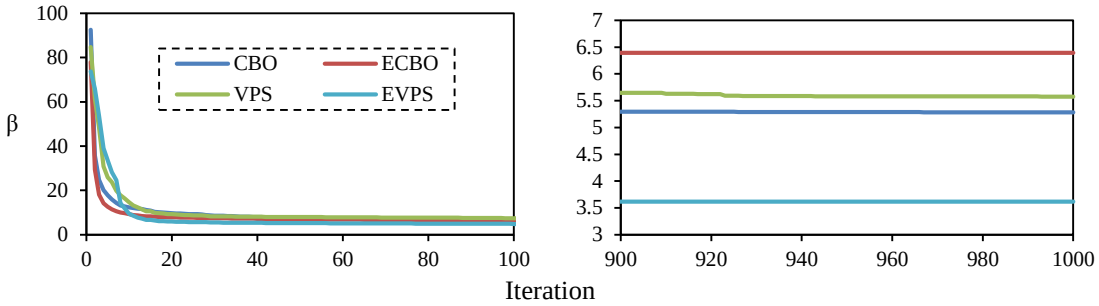

Figure 13. Comparison of the convergence trend of the average runs of each algorithm for the 160-member truss problem

4.4 The 244-bar transmission line tower truss

The last problem is the 244-member truss shown in Fig. 14. This truss is a well-known example that has been studied by many researchers [44-47]. The modulus of elasticity (E) and the density of material (ρ) is 210000 MPa and 276.99 kg / m^3, respectively. The members of this truss are divided into 26 groups. The cross-sectional area of the element group has been selected according to the optimal design of Kaveh et al. [48]. The grouping of elements and their cross-sections are shown in Table 9. The loading condition is shown in Table 10. The number of random variables in this problem is 33 variables. The reliability index for probabilistic constraints is the displacement of the first node in X direction (less than allowable value equal to 3.5 cm).

Fig. 15 shows the performance of the algorithms in 30 independent runs. Diagrams show the ratio of the best total response to each run solution in descending order for each algorithm. The higher the ratio, means the smaller difference between the best answer and the obtained answers which means the better answer is achieved. As shown in this figure, the performance of the EVPS algorithm is more uniform and appropriate relative to other algorithms. The convergence trend of the best response and the average response of each algorithm are shown in Figs. 16 and 17, respectively. The design point, the best, the worst, and the average of the answers of each algorithm and the value of the reliability index obtained from the MCS method for this problem are reported in Table 11. This table shows that the ability of the EVPS algorithm to find the optimal answer (calculating the reliability index) is higher than other algorithms and also, this algorithm has found an answer with an acceptable difference compared to the MCS method.

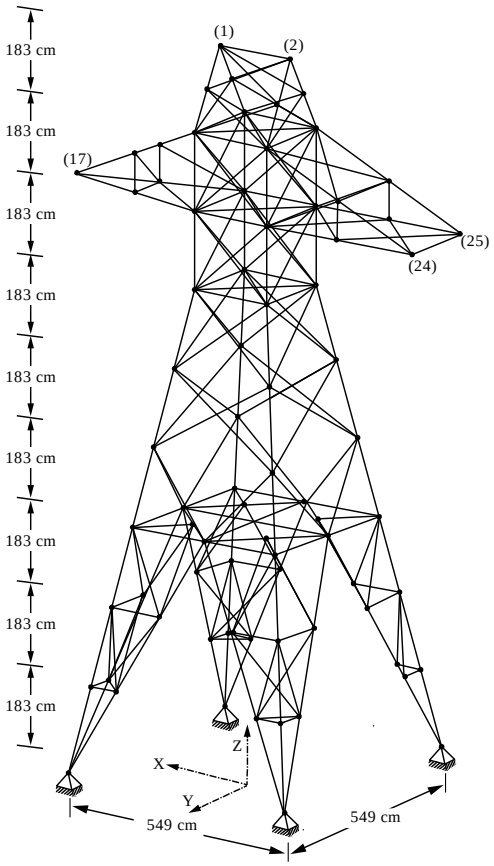

Figure 14. Schematic of the 244-member truss

Table 9: Element grouping adopted in the 244-member truss

Group number	Cross section(cm^2)	Group number	Cross section(cm^2)
1	2.8000	14	3.1226
2	18.4516	15	54.4515
3	5.8193	16	15.4838
4	15.4838	17	3.1226
5	7.0322	18	3.1226
6	26.9677	19	5.8193
7	2.8000	20	51.4838
8	28.1290	21	10.9032
9	5.8193	22	5.8193
10	7.0322	23	5.8193
11	21.3548	24	3.1226
12	23.2903	25	2.8000
13	5.8193	26	2.8000

Table 10: Loading of the 160-member truss

Node	Force in X Direction (kN)	Force in Y Direction (kN)	Force in Z Direction (kN)
1	*P1*=10	*P2*= -30	0.0
2	*P1*=10	*P2*= -30	0.0
17	*P3*=35	*P5*= -90	0.0
24	*P6*=175	*P4*=-45	*0.0*
25	*P6*=175	*P4*=-45	0.0

Table 11: Optimization results obtained by algorithms for the 244-member truss

Random variables of the design point	EVPS	VPS	ECBO	CBO	MSC
A1 (cm^2)	2.7995	2.8235	2.8071	2.8004	-
A2 (cm^2)	18.4310	17.4876	18.3143	18.4655	-
A3 (cm^2)	5.8414	5.8113	6.0193	5.8307	-
A4 (cm^2)	15.4605	16.7594	15.4186	15.4664	-
A5 (cm^2)	7.0339	7.2828	7.0346	7.0360	-
A6 (cm^2)	26.9585	27.1417	26.9677	26.9633	-
A7 (cm^2)	2.8010	2.7488	2.8000	2.7998	-
A8 (cm^2)	28.1326	29.0770	28.1296	28.1289	-
A9 (cm^2)	5.8233	5.9302	5.8193	5.8196	-
A10 (cm^2)	7.0365	7.6462	7.0344	7.0393	-
A11 (cm^2)	21.6208	21.3071	21.0087	21.3099	-
A12 (cm^2)	23.2609	24.1232	23.4674	23.3554	-
A13 (cm^2)	5.8248	6.0087	6.0119	5.8072	-
A14 (cm^2)	3.1233	3.1061	3.1226	3.1226	-
A15 (cm^2)	52.0670	50.7198	55.2426	52.1671	-
A16 (cm^2)	15.5826	15.1558	15.1588	15.2817	-
A17 (cm^2)	3.1230	2.9314	3.1226	3.1187	-
A18 (cm^2)	3.1227	3.1091	3.1226	3.1228	-
A19 (cm^2)	5.8155	5.9927	5.8193	5.8190	-
A20 (cm^2)	48.0287	48.5013	51.8413	49.9866	-
A21 (cm^2)	10.9726	10.6389	10.9506	11.0001	-
A22 (cm^2)	5.8204	5.6356	5.8194	5.8238	-
A23 (cm^2)	5.8184	5.8475	5.8193	5.8188	-
A24 (cm^2)	3.1213	3.1922	3.1226	3.1222	-
A25 (cm^2)	2.8009	2.7067	2.8000	2.7995	-
A26 (cm^2)	2.8001	2.7598	2.8000	2.8004	-
E (MPa)	183393.7815	190722.9282	161014.1243	166426.9122	-
P1 (kN)	10.0586	10.2290	10.5119	9.9376	-
P2 (kN)	30.0089	29.4274	30.0000	29.9981	-
P3 (kN)	34.9044	36.6858	34.3118	34.9411	-
P4 (kN)	45.0205	45.6095	44.9999	44.9957	-

Random variables of the design point	EVPS	VPS	ECBO	CBO	MSC
P5 (kN)	90.0662	92.8943	90.0000	90.0089	-
P6 (kN)	194.3976	201.0994	176.7242	176.7558	-
Best β	3.7449	5.4698	4.9361	4.2931	-
Average β	3.9303	6.1130	5.6067	5.3374	3.6416
Worst β	4.3769	7.3027	7.3630	6.5190	-
Standard deviation β	0.1472	0.4849	0.5479	0.3931	0.0298

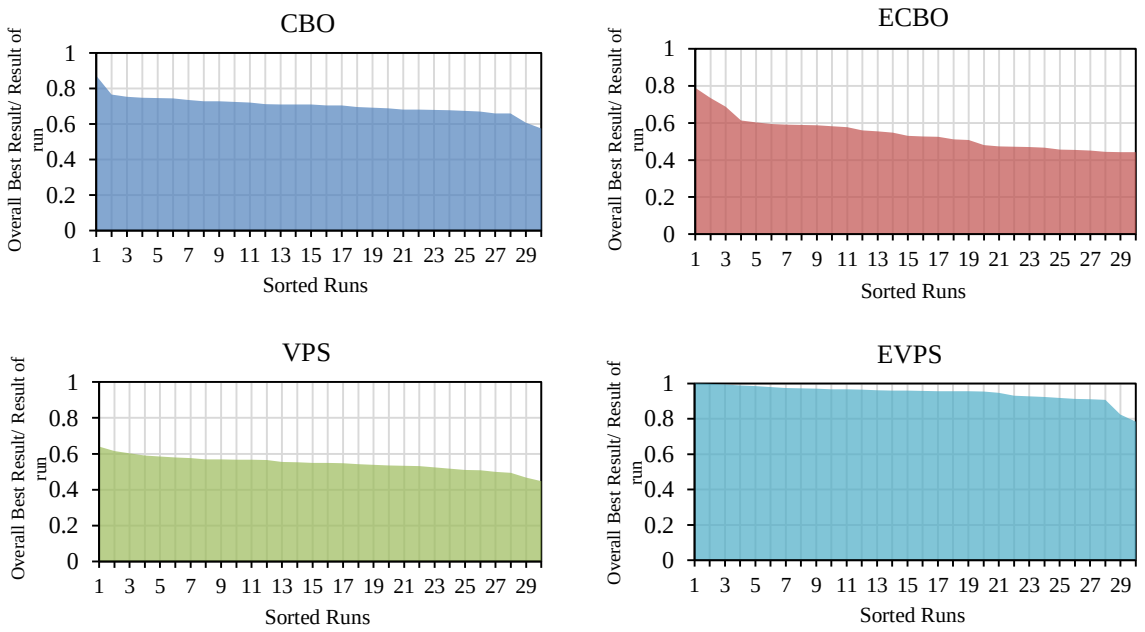

Figure 15. Comparison of the results of all algorithms in 30 independent runs for the 244-member truss problem

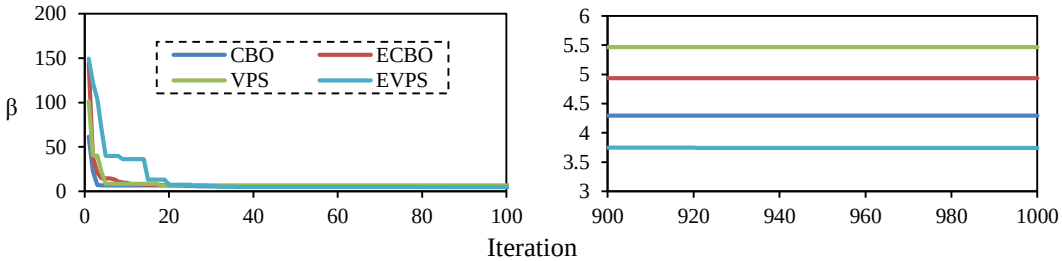

Figure 16. Comparison of the convergence trend of the best run of each algorithm for the 244-member truss problem

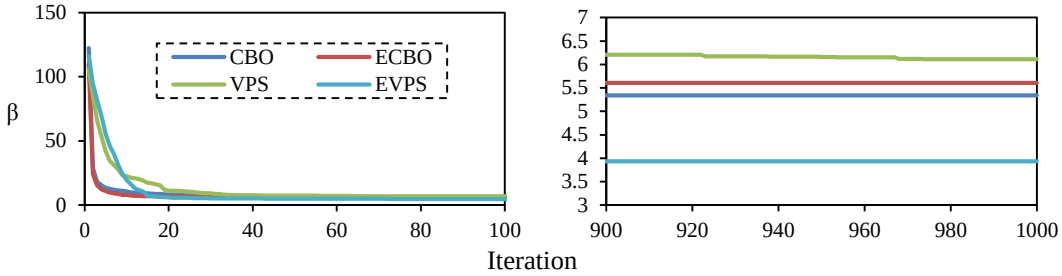

Figure 17. Comparison of the convergence trend of the average runs of each algorithm for the 244-member truss problem

5. CONCLUSION

In this paper, the reliability index of four transmission line tower structures with the probability constraint of nodal displacement was investigated using CBO, ECBO, VPS and EVPS algorithms. The relative difference in the best response of algorithms with the value of the reliability index calculated by the MCS method for problems is between 6 and 13%. The small difference between the results obtained from the algorithms and the results of the MCS method shows that by using metaheuristic algorithms, the reliability index of transmission line tower structures can be calculated with high accuracy. Another advantage of this method is that this approach could be determining the point with the most probability of failure, which is not provided in the MCS. Also, comparing the performance of the algorithms shows the proper and uniform performance of the EVPS algorithm in calculating the reliability index of the studied structures.

REFERENCES

1. Kalatjari V, Kaveh A, Mansoorian P. System reliability assessment of redundant trusses using improved algebraic force method and artificial intelligence, Asian J Civil Eng, 2011; 12(4):423-550.
2. Kaveh A, Dadras Eslamlou A. An efficient method for reliability estimation using the combination of asymptotic sampling and weighted simulation, *Sci Iran, Transact A, Civil Eng* 2019; 26(4): 2108-22.
3. Kaveh A, Javadi SM, Moghanni RM. Reliability analysis via an optimal covariance matrix adaptation evolution strategy: Emphasis on applications in civil engineering, *Period Polytech Civil Eng* 2020; **64**(2): 579-88.
4. Mishra SK, Roy BK, Chakraborty S. Reliability-based-design-optimization of base isolated buildings considering stochastic system parameters subjected to random earthquakes, *Int J Mech Sci* 2013; **75**: 123-33.
5. Wang L, Grandhi RV. Safety index calculation using intervening variables for structural reliability analysis, *Comput Struct* 1996; **59**(6): 1139-48.
6. Lee SH, Kwak BM. Response surface augmented moment method for efficient reliability analysis, *Struct Safe* 2006; **28**(3): 261-72.

7. Zhao YG, Ono T. A general procedure for first/second-order reliability method (FORM/SORM), *Struct Safe* 1999; **21**(2): 95-112.
8. Zhao YG, Ono T. Moment methods for structural reliability, *Struct Safe* 2001; **23**(1): 47-75.
9. Green DK. Efficient markov chain monte carlo for combined subset simulation and nonlinear finite element analysis, *Comput Meth Appl Mech Eng* 2017; **313**: 337-61.
10. Jahani E, Shayanfar MA, Barkhordari MA. A new adaptive importance sampling Monte Carlo method for structural reliability, *KSCE J Civil Eng* 2013; **17**(1): 210-5.
11. Naess A, Leira B, Batsevych O. System reliability analysis by enhanced Monte Carlo simulation, *Struct Safe* 2009; **31**(5): 349-55.
12. Schueller G. Efficient Monte Carlo simulation procedures in structural uncertainty and reliability analysis-recent advances, *Struct Eng Mech* 2009; **32**(1): 1-20.
13. Yonezawa M, Okuda S, Kobayashi H. Structural reliability estimation based on quasi ideal importance sampling simulation, *Struct Eng Mech* 2009; **32**(1): 55-69.
14. Deng L, Ghosn M, Shao S. Development of a shredding genetic algorithm for structural reliability, *Struct Safe* 2005; **27**(2): 113-31.
15. Elegbede C. Structural reliability assessment based on particles swarm optimization, *Struct Safe* 2005; **27**(2): 171-86.
16. Hoseini Vaez SR, Mehanpour H, Fathali MA. Reliability assessment of truss structures with natural frequency constraints using metaheuristic algorithms, *J Build Eng* 2020; **28**: 101065.
17. Kaveh A, Ilchi Ghazaan M. Structural reliability assessment utilizing four metaheuristic algorithms, *Int J Optim Civil Eng* 2015; **5**(2): 205-25.
18. Kaveh A, Massoudi M, Bagha MG. Structural reliability analysis using charged system search algorithm, *Iranian J Sci Technol, Transact Civil Eng* 2014; **38**(C2): 439.
19. Valian E, Tavakoli S, Mohanna Sh, Haghi A. Improved cuckoo search for reliability optimization problems, *Comput Indust Eng* 2013; **64**(1): 459-68.
20. Zou D, Gao L, Li S, Wu J. An effective global harmony search algorithm for reliability problems, *Expert Syst Applicat* 2011; **38**(4): 4642-8.
21. Zou D, Gao L, Wu J, Li S, Li Y. A novel global harmony search algorithm for reliability problems, *Comput Indust Eng* 2010; **58**(2): 307-16.
22. Cornell CA. A probability-based structural code, in *J Proceed* 1969.
23. Hasofer AM, Lind NC. Exact and invariant second-moment code format, *J Eng Mech Div* 1974; **100**(1): 111-21.
24. Kaveh A, Mahdavi VR. Colliding bodies optimization: A novel meta-heuristic method, *Comput Struct* 2014; **139**: 18-27.
25. Kaveh A, Ilchi Ghazaan M. Enhanced colliding bodies optimization for design problems with continuous and discrete variables, *Adv Eng Softw* 2014; **77**: 66-75.
26. Kaveh A, Ilchi Ghazaan M. A new meta-heuristic algorithm: vibrating particles system, *Sci Iran* 2017; **24**(2): 551-66.
27. Kaveh A, Hoseini Vaez S, Hosseini P. MATLAB code for an enhanced vibrating particles system algorithm, *Int J Optim Civil Eng* 2018; **8**(3): 401-14.
28. Kaveh A, Hoseini Vaez SR, Hosseini P. Enhanced vibrating particles system algorithm for damage identification of truss structures, *Sci Iran* 2019; **26**(1): 246-56.
29. Kaveh A, Dadras Eslamlou A. Optimal design of steel curved roof frames by enhanced vibrating particles system algorithm, *Period Polytech Civil Eng* 2019; **63**(4): 947-60.

30. Degertekin SO, Lamberti L, Ugur IB. Discrete sizing/layout/topology optimization of truss structures with an advanced Jaya algorithm, *Appl Soft Comput* 2019; **79**: 363-90.
31. Ho-Huu V, Nguyen-Thoi T, Le-Anh L, Nguyen-Trang T. An effective reliability-based improved constrained differential evolution for reliability-based design optimization of truss structures, *Adv Eng Softw* 2016; **92**: 48-56.
32. Ahrari A, Atai AA, Deb K. Simultaneous topology, shape and size optimization of truss structures by fully stressed design based on evolution strategy, *Eng Optim* 2015; **47**(8): 1063-84.
33. Degertekin SO, Lamberti L, Ugur IB. Sizing, layout and topology design optimization of truss structures using the Jaya algorithm, *Appl Soft Comput* 2018; **70**: 903-28.
34. Husseinzadeh Kashan A, Jalili S, Karimiyan S. Premier league championship algorithm: A multi-population-based algorithm and its application on structural design optimization, in *Socio-Cultur Inspired Metaheurist*, AJ Kulkarni, et al., Editors, Springer Singapore: Singapore, 2019; 215-40.
35. Mortazavi A, Toğan V. Simultaneous size, shape, and topology optimization of truss structures using integrated particle swarm optimizer, *Struct Multidisc Optim* 2016; **54**(4): 715-36.
36. Panagant N, Bureerat S. Truss topology, shape and sizing optimization by fully stressed design based on hybrid grey wolf optimization and adaptive differential evolution, *Eng Optim* 2018; **50**(10): 1645-61.
37. Lee KS, Geem ZW, Lee S-H, Bae K-W. The harmony search heuristic algorithm for discrete structural optimization, *Eng Optim* 2005; **37**(7): 663-84.
38. Barbosa HJC, Lemonge ACC, Borges CCH. A genetic algorithm encoding for cardinality constraints and automatic variable linking in structural optimization, *Eng Struct* 2008; **30**(12): 3708-23.
39. Do DTT, Lee J. A modified symbiotic organisms search (MSOS) algorithm for optimization of pin-jointed structures, *Appl Soft Comput* 2017; **61**: 683-99.
40. Ho-Huu V, Hartjes S, Visser HG, Curran R. An improved MOEA/D algorithm for bi-objective optimization problems with complex Pareto fronts and its application to structural optimization, *Expert Syst Applicat* 2018; **92**: 430-46.
41. Ho-Huu V, Nguyen-Thoi T, Vo-Duy T, Nguyen-Trang T. An adaptive elitist differential evolution for optimization of truss structures with discrete design variables, *Comput Struct* 2016; **165**: 59-75.
42. Jalili S, Husseinzadeh Kashan A. Optimum discrete design of steel tower structures using optics inspired optimization method, *Struct Des Tall Special Build* 2018; **27**(9): e1466.
43. Groenwold AA, Stander N. Optimal discrete sizing of truss structures subject to buckling constraints, *Struct Optim* 1997; **14**(2): 71-80.
44. Kaveh A, Shojaee S. Optimal design of skeletal structures using ant colony optimization, *Int J Numer Method Eng* 2007; **70**(5): 563-81.
45. Saka MP. Optimum design of pin-jointed steel structures with practical applications, *J Struct Eng* 1990; **116**(10): 2599-2620.
46. Toğan V, Daloğlu AT. Optimization of 3D trusses with adaptive approach in genetic algorithms, *Eng Struct* 2006; **28**(7): 1019-27.
47. Toğan V, Daloğlu AT. An improved genetic algorithm with initial population strategy and self-adaptive member grouping, *Comput Struct* 2008; **86**(11): 1204-18.

48. Kaveh A, Talatahari S. Particle swarm optimizer, ant colony strategy and harmony search scheme hybridized for optimization of truss structures, *Comput Struct* 2009; **87**(5): 267-83.